Check for updates

Original Article

Structural Health Monitoring
1–18
© The Author(s) 2024
Article reuse guidelines:
sagepub.com/journals-permissions
DOI: 10.1177/14759217231225402
journals.sagepub.com/home/shm

Unsupervised damage assessment under varying ambient temperature based on an adjusted artificial neural network and new multivariate covariance-based distances

Ali Nikdel and Hashem Shariatmadar

Abstract

Temperature variability is one of the critical environmental conditions that causes confusing changes in structural properties and dynamic responses of bridges similar to damage. In this case, false alarms and mis-detection are among the major errors in health monitoring of such civil structures. High damage detectability is another significant challenge in bridge health monitoring. To deal with these issues, this article proposes an unsupervised damage assessment technique comprising two steps of data normalization and novelty detection. For the first step, an adjusted artificial neural network is considered to remove the effects of temperature variability from dynamic features (modal frequencies). This process is carried out by an auto-associative neural network by adjusting its hidden layer neurons through a new hyperparameter selection algorithm. Using normalized features obtained from the first step, this article proposes three multivariate covariance-based distances called linear dissimilarity analysis, multivariate Kullback–Leibler divergence, and multivariate Bregman distance to compute damage indices or novelty scores for damage assessment. The fundamental principles of these distances lie in three aspects: dividing the normalized features into segments, estimating the covariances of segmented feature sets, and incorporating the estimated covariances into the proposed distance measures. The major contributions of this article include proposing three non-parametric distance measures and developing an unsupervised data normalization framework via a new hyperparameter tuning algorithm for adjusting an artificial neural network. A concrete box-girder bridge is considered to verify the proposed approach, along with several comparative studies. Results show that the method presented here can mitigate severe temperature variability and increase damage detectability with superiority over some traditional and state-of-the-art damage assessment techniques.

Keywords

Structural health monitoring, temperature variability, auto-associative neural network, data normalization, multivariate distance

Introduction

Civil structures, such as bridges, high-rise buildings, dams, and tunnels, are prominent structural systems that play crucial roles in every society. Such structures are often exposed to various natural and man-made excitation sources, including aging, material deterioration, and construction errors that may have adverse influences on structural behavior and lead to damage and even catastrophic events such as collapse. In order to protect civil structures against any unfavorable incident, structural health monitoring (SHM) has become a great necessity for damage assessment and disaster mitigation.[1]

Generally, an SHM program can be implemented by two categories: model-based and data-based methods. A model-based SHM technique relies on constructing an elaborate numerical (finite element) model of a civil structure and utilizing fundamental dynamic principles

Department of Civil Engineering, Faculty of Engineering, Ferdowsi University of Mashhad, Mashhad, Razavi Khorasan, Iran

Corresponding author:
Hashem Shariatmadar, Professor, Department of Civil Engineering, Faculty of Engineering, Ferdowsi University of Mashhad, Azadi Square, Mashhad, Razavi Khorasan 9177948974, Iran.
Email: shariatmadar@um.ac.ir

for damage detection, localization, and quantification[2,3] based on the concept of finite element model updating.[4] Recently, the application of data-based SHM methods has gained increasing attention due to their advantages against model-based techniques,[5] particularly for early assessment of damage.[6] A data-based method mainly lies in directly using raw measured data based on the paradigm of statistical pattern recognition[7] without any finite element modeling and updating. In the context of SHM, this paradigm consists of four steps: operational evaluation, sensing and data acquisition, feature extraction, and feature classification. Sensing and data acquisition can be performed by various devices from conventional sensors (Lynch et al., 2022)[8] and next-generation sensors such as digital cameras (Feng and Feng, 2018)[9] and even smartphones (Sarmadi et al., 2023).[10] Apart from the first two steps, the success in SHM depends strongly on feature extraction and feature classification.

Feature extraction is a process for discovering meaningful information from raw measured data, while feature classification utilizes such information to correctly classify the labels of extracted features. For health monitoring of civil structures, statistical features extracted from different time series models[11–13] and modal properties (i.e., dynamic features) obtained from operational modal analysis (OMA)[14,21] are among the prominent and useful information. Moreover, machine learning is the main methodology for feature classification. This methodology principally aims at developing an intelligent model by using a set called training data and then conducting different tasks such as classification, prediction, clustering, and novelty detection. Depending on the labels of training data, machine learning is categorized as supervised, semi-supervised, and unsupervised learning. Recently, Malekloo et al.[5] comprehensively reviewed applications of these machine learning algorithms to SHM. Moreover, Entezami et al.[14] investigated the pros and cons of such algorithms. An important note about applications of machine learning to SHM is that it may not be necessary to prepare fully or partially labeled training data, which are needed for supervised and semi-supervised learning, for early damage assessment of a civil structure. This means that this strategy can be implemented by unsupervised learning in terms of novelty (anomaly) detection.[15]

Recently, innovative novelty detection techniques have been proposed to assess the occurrence of damage in civil structures. Cha and Wang[16] took advantage of density peaks fast clustering algorithm with some improvements to establish a novelty detector for damage detection and localization. Daneshvar and Sarmadi[17] proposed a novel information-based novelty detection method by getting ideas from the main concepts of density peaks clustering for early damage assessment of bridge structures under short- and long-term monitoring programs. Entezami et al.[18] developed a non-parametric novelty detector in the light of empirical machine learning for damage detection in bridges. Entezami et al.[19] put forward the novel idea of unsupervised meta-learning and developed a locally robust novelty detector based on the Mahalanobis-squared distance (MSD) for bridge damage assessment. Zhou et al.[20] researched dam safety assessment by the concept of novelty detection. They suggested a generative adversarial network and a variational auto-encoder to develop a novelty detector by considering data-level anomaly detection and information fusion. Sarmadi et al.[21] proposed a novel probabilistic novelty detection method based on the idea of self-data clustering and semi-parametric extreme value theory. Entezami et al.[22] proposed a novel non-parametric novelty detector based on local outlier factors and a self-adaptive neighbor searching algorithm for detecting early damage in bridge structures.

Despite development of various unsupervised novelty detection techniques for SHM, an important challenge in SHM is the ability to yield discriminative novelty scores for increasing detectability of damage. The other critical challenge, which also affects the performances of novelty detectors, is the existence of environmental and/or operational variability.[23] This is because the environmental and operational conditions can directly affect and change inherent properties of a civil structure (i.e., the mass, stiffness, and damping) and also structural responses (e.g., modal data). Temperature variability is one of the critical environmental conditions with profound impacts on bridge structures, especially in long-term monitoring.[24] One of these impacts relates to temperature variations in freezing weather, which can strongly affect structural stiffness and significantly increase modal frequencies. It was observed in some research studies that such deceptive variability can mask real adverse changes caused by damage in different civil structures.[19,25] Because the effects of environmental and/or operational variability resemble structural damage, false alarm (false positive) and mis-detection (false negative) are among the most critical errors in SHM under the concept of unsupervised novelty detection.[26] The false alarm and mis-detection errors are directly related to economic and safety issues; thus, it is essential to remove such deceptive conditions from structural features.

In the context of SHM, data normalization is the main methodology for eliminating or mitigating the effects of environmental and/or operational variability conditions.[23] Totally, this methodology is categorized as input-output or output-only approaches. The former

is based on measuring both the environmental/operational data (e.g., temperature) and structural responses/features (e.g., modal frequencies) under the concept of supervised learning, while the latter depends only on the structural responses based on the framework of unsupervised learning. For the input-output data normalization, the main purpose is to develop a regression model to represent the relationship between the measured environmental/operational (input) and response (output) data and then extract the model residuals as the normalized responses/features.[27–32] Despite the applicability of such data normalization techniques, it may not be possible to measure all influential input variables.[32,33] Therefore, it seems that the output-only data normalization is more beneficial for removing the environmental and/or operational variability. For this reason, valuable research studies were conducted to develop innovative unsupervised data normalization techniques.[34–38]

One of the most effective and tried-and-tested unsupervised data normalization methods is based on auto-associative neural networks (AANNs).[39] This is because such models are suitably resilient to noise and any source of variability in data.[40] An AANN conforms to a feed-forward back-propagation configuration and generates an unsupervised neural network with five layers, that is, an input layer, three hidden layers called mapping, bottleneck, and de-mapping, and an output layer. Figueiredo et al.[41] investigated the AANN-aided data normalization for removing simulated environmental and operational conditions in a laboratory frame by using statistical (time series) features obtained from a time series model. Zhou et al.[42] also presented an AANN model for damage detection with the focus on avoiding false alarms and false detection results caused by the effects of environmental and/or operational variability. Regardless of the neurons of the bottleneck layer, they proposed three different hyperparameter selection methods based on validation data error, Akaike information criterion, final prediction error, and Bayesian regularization to choose the neurons of mapping and de-mapping layers. Gu et al.[43] adopted a modified AANN as a data normalization model for removing the temperature variability from modal frequencies. Similarly, they attempted to find the most appropriate neuron sizes of the mapping and de-mapping layers by considering a constant neuron for the bottleneck layer. Although the application of the AANN to data normalization is satisfactory, an inappropriate hyperparameter selection, particularly ignoring the number of neurons of the bottleneck layer, may affect its performance and lead to erroneous results. For this drawback, Sarmadi[40] proposed an iterative method to select the neuron sizes of all hidden layers of the AANN and extract normalized features for bridge damage assessment via two non-parametric novelty detectors. However, the major limitation of that method is its dependency on the outputs of novelty detectors.

To address the aforementioned limitations and challenges, this article is intended to propose a new unsupervised damage assessment technique under strong temperature variability. This technique consists of two steps: data normalization and novelty detection. For the first step, as discussed, we take advantage of the AANN-oriented data normalization. Thanks to knowing the number of hidden layers of this artificial neural network, a new hyperparameter selection approach is proposed to determine the neuron sizes of the mapping, bottleneck, and de-mapping layers with the emphasis on removing the temperature variations. Indeed, this approach is an improvement on the hyperparameter selection proposed by Sarmadi[40] so that the proposed approach can choose the optimum number of neurons of each hidden layer directly from data. For the second step, this article proposes three multivariate covariance-based distances called linear dissimilarity analysis (LDA), multivariate Kullback-Leibler divergence (MKLD), and multivariate Bregman divergence (MBD). The crux of these distance measures is to use a non-parametric feature segmentation for dividing entire sets of features of undamaged and damaged conditions into low-dimensional segments and estimating covariances of these segments, which serve as the main factors for distance calculations. Finally, the dissimilarity between two pair segments is computed by each of the proposed distance measures to determine novelty scores for damage assessment. The major contributions/innovations of this article include proposing different distance-based novelty detectors with a non-parametric feature segmentation and enhancing an AANN-aided data normalization algorithm in conjunction with a new hyperparameter selection strategy. The great advantages of the approaches presented in this article can be summarized as removing the impacts of strong environmental variability, increasing detectability of damage, and reducing false alarm and misdetection errors. A concrete box-girder bridge, that is, the Z24 bridge, along with its long-term modal frequencies, is considered to verify the effectiveness and reliability of the proposed unsupervised damage assessment technique. Several comparative studies are also conducted to prove the superiority of this technique over some traditional and state-of-the-art unsupervised approaches. Results show that the proposed AANN-aided date normalization, in conjunction with its hyperparameter selection algorithm is able to effectively remove the deceptive changes in the bridge modal frequencies caused by strong temperature variability. It is also observed that the proposed covariance-

based distance measures succeed in detecting damage with low-dimensional features and high damage detectability.

Data normalization

Since the environmental and/or operational variability seriously affects the outcomes of a real-world SHM project, especially in a long-term monitoring program, data normalization is mandatory for ensuring the final decision. Accordingly, one should attempt to remove variations caused by environmental and/or operational conditions from structural responses/features. Having considered the benefits of output-only data normalization, this section briefly describes how an unsupervised artificial neural network such as the AANN can provide normalized features for damage assessment.

Assume that $\mathbf{X}$ is the matrix of feature (training) samples regarding the normal (undamaged) condition of a civil structure during the training/baseline period. It is also considered that this matrix consists of n samples (observations) and m variables. For the modal frequency-based damage assessment, n and m denote the numbers of modal frequencies and modes, respectively. Accordingly, one initially needs to develop an AANN by inputting the training data $\mathbf{X}$ and tuning the neurons of its hidden layers. Subsequently, the network output $\hat{\mathbf{X}}$ is extracted from the output layer of the AANN. Finally, the residual between the input and output data is determined as the normalized version of the training data. Indeed, the influences of environmental and/or operational variability in the original (training) data are excluded from the residual data.

During the inspection phase, when the state of the civil structure is unknown, one needs to perform the same residual extraction strategy with a difference. This difference relates to model development. In other words, in contrast to the training/baseline stage, it is not necessary to develop any AANN. In this case, it suffices to use the trained model (AANN) in the training phase and determine the residual data of the model input and output. However, it should be noted that the input data in the inspection stage contains the testing features concerning the current state of the civil structure. Suppose that these features are collected to make the testing matrix $\mathbf{Z}$, including k samples and m variables. Using the trained AANN, the testing data is fed into the network to determine the output matrix $\hat{\mathbf{Z}}$. Eventually, the residual between $\mathbf{Z}$ and $\hat{\mathbf{Z}}$ is extracted as the normalized version of the testing data.

Auto-associative neural network

The AANN is one of the tried-and-tested artificial neural networks that aims to produce an approximation of mapping between the network inputs and outputs by using a feed-forward connection and different transfer functions and back-propagation training algorithms.[39] The network learns a mapping from given inputs to desired outputs by adjusting internal weights to minimize the error of an objective function. The AANN consists of five layers, including an input layer, three hidden layers called mapping, bottleneck, and de-mapping, and an output layer. The input layer receives the original features, which can include the environmental and/or operational variability conditions. The output layer returns the normalized or filtered version of the original features. An important note about the topology of the AANN is that the bottleneck layer, which plays the key role in the functionality of the AANN, should have smaller neurons than the other hidden layers.[39] The great merits of the AANN can be summarized as it can provide an unsupervised learning framework without any labeled information and also remove noise, outliers, and any variability source from features.

The AANN is viewed as a coupling of two single-hidden layer networks. The input, mapping, and bottleneck layers generate the first network by employing the nonlinear function G aiming at projecting the feature samples (inputs) to a lower dimension space. This mapping is expressed as follows:

$$\mathbf{b}_i = G_i(\mathbf{x}), \quad \forall i = 1, 2, ..., h \tag{1}$$

where $\mathbf{b}_i$ denotes the output of the ith bottleneck node, h represents the number of nodes (neurons) of the bottleneck layer, and $\mathbf{x} = \{x_1,\ldots,x_n\}$ is the vector of the n-dimensional feature samples (inputs). The bottleneck, de-mapping, and output layers make the second network by utilizing the other nonlinear function H that reproduces an approximation of the inputs from the factors at the output of the bottleneck layer in the following form:

$$\hat{\mathbf{x}}_j = H_j(\mathbf{b}), \quad \forall j = 1, 2, ..., n \tag{2}$$

Using all feature vectors in the input feature matrix $\mathbf{X} = [\mathbf{x}_1,\ldots,\mathbf{x}_m]^{\mathrm{T}}$, where each vector consists of n samples, the AANN gives the output feature matrix $\hat{\mathbf{X}} = [\hat{\mathbf{x}}_1,\ldots,\hat{\mathbf{x}}_m]^{\mathrm{T}}$. Hence, it can be removed possible environmental and/or operational variability in the original or input feature set ($\mathbf{X}$) by computing the absolute difference between $\mathbf{X}$ and $\hat{\mathbf{X}}$. For the jth feature sample concerning the undamaged condition, the residual (feature) vector is given by:

$$\mathbf{e}_{\mathbf{x}_j} = \mathbf{x}_j - \hat{\mathbf{x}}_j \tag{3}$$

Having considered all n feature samples, $\mathbf{E}_{\mathbf{x}} = [\mathbf{e}_{\mathbf{x}_1},\ldots,\mathbf{e}_{\mathbf{x}_m}]^{\mathrm{T}}$ is the normalized feature matrix of the

undamaged state. Utilizing the trained AANN, the same process can be implemented to extract the normalized feature matrix of the current structural condition; that is, $\mathbf{E_z} = [\mathbf{e}_{\mathbf{z}_1},\ldots,\mathbf{e}_{\mathbf{z}_m}]^{\mathrm{T}}$. Each of the vectors of this matrix can be expressed as follows:

$$\mathbf{e}_{\mathbf{z}_l} = \mathbf{z}_l - \hat{\mathbf{z}}_l \tag{4}$$

where $l = 1,\ldots,k$. It is worth remarking that although the training data (i.e., the input feature matrix $\mathbf{X}$) fed into the AANN relates to the undamaged state, this label may contain other undamaged cases. During the training phase, it is considered that all feature samples belong to the undamaged condition; however, it is not clear which features are exactly influenced by which types of environmental and/or operational conditions. On the other hand, some variability conditions have similar impacts on structural responses or features.[23] Under such circumstances, there may exist various unknown conditions of environmental and/or operational changes, which can affect the training data but their labels are unknown. For these reasons, the process of data normalization via the AANN conforms to an unsupervised learning framework.

Hyperparameter selection

In machine learning, the process of hyperparameter selection (optimization) is the utmost importance for tuning or choosing unknown components of a parametric model. Such components are known as *hyperparameters* because they control the learning procedure and affect the model performance. For artificial neural networks, the numbers of hidden layers and neurons are the main hyperparameters that should be determined properly.[40] In most cases, an AANN with three hidden layers is sufficient; hence, it is not essential to specify the number of hidden layers implying one of the advantages of this network. Moreover, the neuron sizes of the input and output layers are known, in which case the remaining hyperparameters are the neuron numbers of the mapping, bottleneck, and de-mapping layers. According to Kramer's suggestion, these neurons should be large enough to ensure adequate representational capacity without the occurrence of overfitting problems.[39] To prevent this problem, the following inequality, which limits the number of adjustable neurons of the AANN, should be held:

$$l_1 + l_2 < \frac{m(n-h)}{m+h+1} \tag{5}$$

where l_1 and l_2 are the numbers of neurons for the mapping and de-mapping layers, respectively. Although the utilization of Equation (5) helps us to control the overfitting problem; the accurate choice of the unknown components l_1, l_2, and h is more important. Despite suggesting some techniques for determining these hyperparameters,[42,43] mainly focused on the neurons of the mapping and de-mapping layers. Furthermore, the hyperparameter selection approach proposed by Sarmadi[40] relies on the outputs of novelty detection. Hence, the development of this strategy is essential.

The main rationale behind using the AANN is to remove the effects of environmental and/or operational variability from structural features. Therefore, it is attempted to select the neurons of the hidden layers such that the deceptive variations stemming from the environmental and/or operational conditions have less influence on the structural features. Another important note is that one assumes that the features of the normal condition, which make the training data for modeling

Algorithm 1. Selection of neurons of hidden layers of an AANN

Initialization

X_int=Input matrix;
l_max=Number of the maximum sample neurons for the mapping and de-mapping layers;
h_max= Number of the maximum sample neurons for the bottleneck layer;
trainFcn=Training algorithm (Default: *Levenberg-Marquardt backpropagation*);
for i=1:h_max **do**
  for j=1:l_max **do**
    - Design an AANN with *j* sample neurons for the mapping and de-mapping layers and *i* sample neurons for the bottleneck layer.
    - Train the AANN by the input matrix X_int, the *i* and *j* sample neurons, and the pre-defined training algorithm.
    - Obtain the network output X_out at the output layer of the trained AANN.
    - Determine the residual matrix of the input and output matrices.
    - Calculate the Euclidean norm of the residual matrix.
    - Store the norm value of the i^{th} and j^{th} sample neurons in a norm matrix.
  end
end

Finalization

- Find the minimum norm value of the norm matrix, which is comprised of h_max rows and l_max columns.
- h_opt=Optimal neuron number of the bottleneck layer, which is the row of the norm matrix with the minimum norm value.
- l_opt=Optimal neuron number of the mapping and de-mapping layers, which is the column of the norm matrix with the minimum norm value
- Check the neuron inequality equation for avoiding the overfitting problem. If the equation does not hold, change l_max and h_max on condition that l_max>h_max and then repeat Algorithm 1.

the AANN, can cover all possible environmental and/or operational variability (e.g., 1-year measurement or monitoring scheme).[44]

Given the training matrix $\mathbf{X}$, the main objective is to develop an iterative algorithm by learning AANNs with various sample neurons of the hidden layers and checking the algorithm output via a criterion. In this article, the Euclidean norm of the residual matrix is suggested as the criterion of interest for hyperparameter selection. Because the norm value of the residual matrix is a metric for measuring the difference between the input and output of the AANN (i.e., $\mathbf{X}$ and $\hat{\mathbf{X}}$), a small norm value means that there is no considerable difference between the input and output matrices. In this regard, the improvement or change of the hyperparameters (i.e., the neuron sizes) may not have progressed. Thus, one can infer that the small norm of the residual matrix is representative of the low effect of the environmental and/or operational conditions. It should be mentioned that the AANN used in the process of data normalization has a symmetric configuration in its hidden layers, in which case the mapping and de-mapping layers have the same neurons; that is, $l_1 = l_2 = l$. Moreover, one should ensure that the number of neurons regarding the bottleneck layer is smaller than the mapping and de-mapping layers (i.e., $l > h$). For the sake of convenience, Algorithm 1 presents the pseudo-code of the proposed hyperparameter selection.

Multivariate covariance-based distance measures

Linear dissimilarity analysis

The LDA is a multivariate distance measure for dissimilarity analysis, which was initially proposed by Kano et al.[45] in the field of chemical engineering. The main index for dissimilarity analysis in the LDA is to estimate the covariance matrix of two multivariate datasets and then decompose this matrix. Assume that $\mathbf{X}_1$ and $\mathbf{X}_2$ are two matrices including n_1 and n_2 samples but m variables, where one of the matrices is selected as a reference set and the other one as a target set. The covariance of the mixture of these matrices is given by:

$$\mathbf{R} = \frac{1}{n_1 + n_2} \begin{bmatrix} \mathbf{X}_1 \\ \mathbf{X}_2 \end{bmatrix}^T \begin{bmatrix} \mathbf{X}_1 \\ \mathbf{X}_2 \end{bmatrix} = \frac{n_1}{n_1 + n_2} \mathbf{R}_1 + \frac{n_2}{n_1 + n_2} \mathbf{R}_2 \quad (6)$$

where

$$\mathbf{R}_i = \frac{1}{n_i} \mathbf{X}_i^T \mathbf{X}_i, \quad \forall i = 1, 2 \quad (7)$$

The covariance matrix $\mathbf{R}$ is the central core of the LDA, as it plays the main role in calculating the distance between $\mathbf{X}_1$ and $\mathbf{X}_2$. In the next step, it is necessary to decompose $\mathbf{R}$ via a matrix decomposition technique. Using the eigenvalue decomposition, one can obtain:

$$\mathbf{P}^T \mathbf{R} \mathbf{P} = \mathbf{\Lambda} \quad (8)$$

where $\mathbf{\Lambda}$ is a diagonal matrix whose diagonal components are the eigenvalues of $\mathbf{R}$. Furthermore, $\mathbf{P}$ is an orthogonal matrix on condition that $\mathbf{P}^{\mathrm{T}}\mathbf{P} = \mathbf{I}$, where $\mathbf{I}$ is an identity matrix. Using the matrices $\mathbf{\Lambda}$ and $\mathbf{P}$, one should determine the reconstructed version of the reference set in the following form:

$$\mathbf{Y} = \sqrt{\frac{n_1}{n_1 + n_2}} \mathbf{X}_1 \mathbf{P} \mathbf{\Lambda}^{-1/2} \quad (9)$$

In the following, the diagonal elements of the covariance matrix of $\mathbf{Y}$ are extracted and stored in the m-dimensional vector $\mathbf{w}$ as follows:

$$\mathbf{w} = diag\left(\frac{1}{n_1} \mathbf{Y}^T \mathbf{Y} \right) \quad (10)$$

Eventually, the dissimilarity index (D_L) of the LDA for measuring the distance between $\mathbf{X}_1$ and $\mathbf{X}_2$ is defined as follows[45]:

$$D_L = \frac{4}{m} \sum_{j=1}^{m} \left(w_j - 0.5 \right)^2 \quad (11)$$

where w_j is the jth element of the vector $\mathbf{w}$. The index or novelty score D_L varies between zero and one, which reflects the similar and dissimilar labels between $\mathbf{X}_1$ and $\mathbf{X}_2$. For the problem of damage assessment, $D_L = 0$ and $D_L = 1$ are ideally equivalent to undamaged and damaged conditions, respectively.

Multivariate Kullback-Leibler divergence

In statistics, the Kullback-Leibler divergence (KLD) is a well-known statistical measure for computing the distance between two univariate probability distributions based on a logarithmic function.[46,47] For the probability distributions $\mathbf{p}_1$ and $\mathbf{p}_2$ with p samples, the univariate version of KLD is written as follows:

$$d_{KL}(\mathbf{p}_1 || \mathbf{p}_2) = \sum_{i=1}^{p} \mathbf{p}_1(i) \log \frac{\mathbf{p}_1(i)}{\mathbf{p}_2(i)} \quad (12)$$

For the multivariate feature sets $\mathbf{X}_1$ and $\mathbf{X}_2$, with the mean vectors $\boldsymbol{\mu}_1$ and $\boldsymbol{\mu}_2$ as well as the covariance

matrices $\mathbf{R}_1$ and $\mathbf{R}_2$, it is possible to adopt the multivariate version of KLD for computing their distance in the following form[48]:

$$D_M(\mathbf{X}_1||\mathbf{X}_2) = \frac{1}{2}\left(\log\frac{\det(\mathbf{R}_2)}{\det(\mathbf{R}_1)} - m + \mathrm{tr}\left(\mathbf{R}_2^{-1}\mathbf{R}_1\right) + (\boldsymbol{\mu}_2 - \boldsymbol{\mu}_1)^T\mathbf{R}_2^{-1}(\boldsymbol{\mu}_2 - \boldsymbol{\mu}_1)\right) \quad (13)$$

where "det" and "tr" stand for the determinant and trace of a matrix. Note that the original and well-known version of the MKLD is based on the multivariate probability distributions without directly considering the feature matrices. Therefore, this article employs a different MKLD with a minor modification for damage assessment.

Multivariate Bregman divergence

In mathematics and statistics, a Bregman divergence is a measure of distance between two points defined in terms of a strictly convex function. When the points of interest are interpreted as probability distributions either as quantities of a parametric model or a dataset of an observed value, the Bregman distance is a statistical measure. Considering ϕ as a real-valued strictly convex function, the Bregman divergence with respect to ϕ for two points (vectors) $\mathbf{x}_1$ and $\mathbf{x}_2$ is defined as[49]:

$$D_\phi(\mathbf{x}||\mathbf{y}) = \phi(\mathbf{x}) - \phi(\mathbf{y}) - (\mathbf{x} - \mathbf{y})^T\nabla\phi(\mathbf{y}) \quad (14)$$

It is possible to expand this definition to convex functions defined over matrices. In such a case, given the matrices $\mathbf{X}_1$ and $\mathbf{X}_2$, the MBD is expressed as follows[49]:

$$D_\phi(\mathbf{X}_1||\mathbf{X}_2) = \phi(\mathbf{X}_1) - \phi(\mathbf{X}_2) - tr(\nabla\phi(\mathbf{X}_2)(\mathbf{X}_1 - \mathbf{X}_2)) \quad (15)$$

The properties of the MBD $D_\phi(\mathbf{X}_1||\mathbf{X}_2)$ are determined by the differentiable function ϕ. When this function is selected as a logarithmic function of the determinant of the matrices $\mathbf{X}_1$ and $\mathbf{X}_2$ and the Burg entropy, Equation (15) can be rewritten as follows:

$$D_B(\mathbf{X}_1||\mathbf{X}_2) = tr\left(\mathbf{X}_1\mathbf{X}_2^{-1}\right) - \log\left(\det\left(\mathbf{X}_1\mathbf{X}_2^{-1}\right)\right) - m \quad (16)$$

$D_B(\mathbf{X}_1||\mathbf{X}_2)$ directly measures the distance between the matrices $\mathbf{X}_1$ and $\mathbf{X}_2$ without considering the correlation between their variables. To address this limitation, one can expand Equation (16) to define the covariance-based MBD in the following form:

$$D_B(\mathbf{X}_1||\mathbf{X}_2) = tr\left(\mathbf{R}_1\mathbf{R}_2^{-1}\right) - \log\left(\det\left(\mathbf{R}_1\mathbf{R}_2^{-1}\right)\right) - m \quad (17)$$

In contrast to Equation (16), the covariance matrices of $\mathbf{X}_1$ and $\mathbf{X}_2$ are incorporated into the MBD allowing it to consider the correlation between the variables of $\mathbf{X}_1$ and $\mathbf{X}_2$.

Proposed SHM technique

Once the normalized features are extracted from the AANN, those are applied to the proposed covariance-based distance measures for novelty detection. The main part of the proposed SHM technique is to divide the normalized feature matrices $\mathbf{E_x}$ and $\mathbf{E_z}$ into segments (sub-matrices) with equal dimensions (samples). Note that all segments include the same variables (m) as the matrices $\mathbf{E_x}$ and $\mathbf{E_z}$. First, the distance calculation through the proposed multivariate measures is performed to determine the dissimilarity between two segments regarding the normal condition. Suppose that the matrix $\mathbf{E_x}$ is divided into c segments with s samples and m variables; that is, $\mathbf{E_x} = [\mathbf{E_x}^{(1)}\ldots\mathbf{E_x}^{(c)}]$. On this basis, the cumulative distance of the ith segment with respect to the jth segment is given by:

$$D\left(\mathbf{E_x}^{(i)}\right) = \sum_{j=1}^{c} D\left(\mathbf{E_x}^{(i)}||\mathbf{E_x}^{(j)}\right), \quad \forall i = 1, 2, ..., c \quad (18)$$

where $D(\mathbf{E_x}^{(i)}||\mathbf{E_x}^{(j)})$ stands for the distance between the ith and jth segments of $\mathbf{E_x}$, and the term "D" refers to each of the LDA, MKLD, and MBD measures. Considering all segments, one can make a vector of c distance values as $\mathbf{d}_{nor} = [D(\mathbf{E_x}^{(1)})\ldots D(\mathbf{E_x}^{(c)})]$ regarding the normal condition of the civil structure evaluated in the training stage.

Second, the feature matrix $\mathbf{E_z}$ is divided into r segments with s samples and m variables; that is, $\mathbf{E_z} = [\mathbf{E_z}^{(1)}\ldots\mathbf{E_z}^{(r)}]$. Subsequently, the distance calculation is carried out to measure the dissimilarity between the segments of $\mathbf{E_x}$ and $\mathbf{E_z}$. Accordingly, the distance between each segment of $\mathbf{E_z}$ and $\mathbf{E_x}$ is computed to make a cumulative distance as follows:

$$D\left(\mathbf{E_z}^{(i)}\right) = \sum_{j=1}^{c} D\left(\mathbf{E_z}^{(i)}||\mathbf{E_x}^{(j)}\right), \quad \forall i = 1, 2, ..., r \quad (19)$$

where $D(\mathbf{E_z}^{(i)}||\mathbf{E_x}^{(j)})$ denotes the distance between the ith segment of $\mathbf{E_z}$ and jth segment of $\mathbf{E_x}$. Using all segments of $\mathbf{E_z}$, it is possible to produce a vector of r distance values regarding the current state of the structure $\mathbf{d}_{\mathrm{cur}} = [D(\mathbf{E_z}^{(1)})\ldots D(\mathbf{E_z}^{(r)})]$. The distance quantities in this vector are then compared with the distance values of $\mathbf{d}_{\mathrm{nor}}$ for damage detection. In order to increase the reliability of damage detection, the best solution is to estimate a threshold.[6,50] This procedure is usually performed by using the outputs of the normal (undamaged) condition. Hence, the distance amounts in $\mathbf{d}_{\mathrm{nor}}$ are applied to estimate a threshold on the basis of the

Algorithm 2. Proposed SHM approach

Initialization

Ex=Input matrix including the normalized feature samples regarding the normal condition;
Ez=Input matrix including the normalized feature samples regarding the current condition;
n=Number of samples (observations or rows) of Ex;
k=Number of samples (observations or rows) of Ez;
s=Number of samples of each segment (Default: s=10);
c=Number of segments of Ex, where c=round(n/s);
r=Number of segments of Ez, where r=round(k/s);

Segmentation
for i=1:c-1 **do**
- Divide Ex into c-1 segments with s samples by the function $Exc\{i,\ :\} = Ex((i-1)*s+1 : i*s,\ :)$, which is equivalent to $\mathbf{E}_{\mathbf{x}}^{(i)}$.

end
- Construct the last segment of Ex with n−(s×c) samples by the function$Exc\{c,\ :\} = Ex((c-1)*s+1 : end)$, which is equivalent to $\mathbf{E}_{\mathbf{x}}^{(c)}$.

for i=1:r-1 **do**
- Divide Ez into r-1 segments with s samples by the function $Ezr\{i,\ :\} = Ez((i-1)*s+1 : i*s,\ :)$, which is equivalent to $\mathbf{E}_{\mathbf{z}}^{(i)}$.

end
- Construct the last segment of Ez with k−(s×r) samples by the function $Ezr\{r,\ :\} = Ez((r-1)*s+1 : end)$, which is equivalent to $\mathbf{E}_{\mathbf{z}}^{(r)}$.

Distance Calculation for Normal Condition
for i=1:c **do**
- Set Exi as the i^{th} matrix of $Exc\{i,\ :\}$

  for j=1:c **do**
  - Set Exj as the j^{th} matrix of $Exc\{j,\ :\}$
  - Calculate $D(\mathbf{E}_{\mathbf{x}}^{(i)} || \mathbf{E}_{\mathbf{x}}^{(j)})$

  end
  - Determine the cumulative distance $D(\mathbf{E}_{\mathbf{x}}^{(i)})$ by Eq. (15) and construct d_{nor}.

end
Threshold estimation by the distance values in d_{nor} by the 95% confidence interval.

Distance Calculation for Current Condition
for i=1:r **do**
- Set Ezi as the i^{th} matrix of $Exz\{i,\ :\}$, which is equivalent to $\mathbf{E}_{\mathbf{z}}^{(i)}$.

  for j=1:c **do**
  - Set Exj as the j^{th} matrix of $Exc\{j,\ :\}$, which is equivalent to $\mathbf{E}_{\mathbf{x}}^{(j)}$.
  - Calculate $D(\mathbf{E}_{\mathbf{z}}^{(i)} || \mathbf{E}_{\mathbf{x}}^{(j)})$.

  end
  - Determine the cumulative distance $D(\mathbf{E}_{\mathbf{z}}^{(i)})$ by Eq. (16) and make d_{cur}.

end
- Collect the distance values in d_{nor} and d_{cur} into a new vector with c + r samples and compare all distance quantities with the threshold.

probabilistic characteristics of the mentioned distance values.

Under the assumption of Gaussianity of the distances in $\mathbf{d}_{\text{nor}}$, the threshold is estimated by the upper bound of a confidence interval value. Using the 5% significance level, the threshold of interest is based on computing the 95% confidence interval of the distance quantities. The false positive (i.e., false alarm or Type I) error does not occur if and only if no distance value (novelty score) of the normal condition in $\mathbf{d}_{\text{nor}}$ exceeds the threshold limit. In fact, it is expected that all distance quantities of the undamaged condition fall below the threshold line. Any deviation of the distance amount in $\mathbf{d}_{\text{cur}}$ from the estimated threshold is representative of the damage occurrence. The false negative (i.e., mis-detection or Type II) error occurs when any distance quantity of the damaged condition is under the threshold. For the sake of simplicity, all the above-mentioned descriptions are summarized in Algorithm 2.

Application to the Z24 bridge

In this section, long-term modal frequencies extracted from acceleration responses of the Z24 bridge[34] are

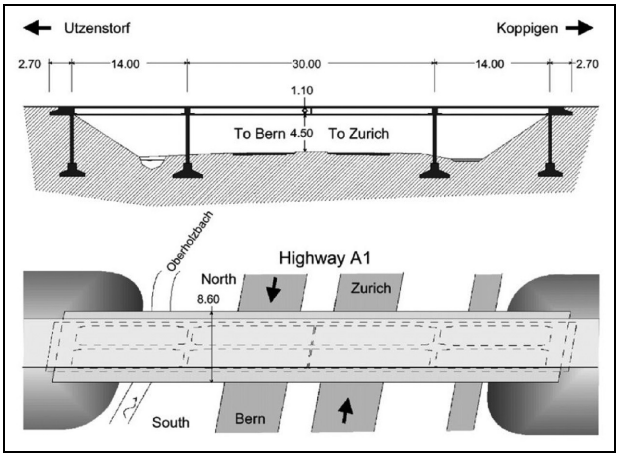

Figure 1. The Z24 bridge.[51]

applied to verify the effectiveness and reliability of the proposed SHM technique. This structure was a classical post-tensioned concrete box-girder bridge built in Switzerland. The structure of the bridge consisted of the main span of 30 m and two side spans of 14 m. Figure 1 shows this bridge and its dimensions. The Z24 bridge was demolished to build a new bridge with a larger side span. Before this event, a long-term continuous monitoring test was performed to capture diverse environmental parameters and acquire acceleration time histories in different positions and directions. During the month before complete demolition, the bridge was gradually subjected to realistic damages in a controlled way.

The structural features for damage assessment are the bridge modal frequencies of four modes, as shown in Figure 2, where the vertical lines separate the normal and damaged conditions. These features include 3932 samples (observations) so that the first 3470 samples are related to the normal condition of the Z24 bridge, and the last 462 samples (3471–3932) are concerned with the damaged state. In Figure 2, the sudden jumps with sharp increases in the modal frequencies of the normal condition obviously indicate their high sensitivity to the environmental (temperature) variability when the air temperature was below 0°C (i.e., freezing weather).[19]

Before the procedures of data normalization and novelty detection, it is necessary to define training and testing datasets. On this basis, the training samples are based on 90% of the modal frequencies regarding the normal condition. In other words, the training data $\mathbf{X}$ is a matrix of 3123 samples (n) and four variables (m). Additionally, the remaining 10% of the modal frequencies of the normal condition (the samples 3124–3470) and all modal frequencies of the damaged state are applied to build the testing data $\mathbf{Z}$, which is a matrix of 809 samples (k) and four variables.

Data normalization

To remove the environmental (temperature) variations from the bridge modal frequencies and prepare normalized features for novelty detection, the process of data normalization is performed by learning an AANN. At first, one needs to determine the neuron sizes of the mapping, bottleneck, and de-mapping layers based on the proposed hyperparameter selection algorithm. This process is performed by only training data, in which case the input matrix used in Algorithm 1 is the matrix $\mathbf{X}$. The maximum sample neurons for the mapping (de-mapping) and the bottleneck layer are set to 30 and 10, respectively. The main goal is to choose the optimal neuron number with the smallest Euclidean norm value of the residual matrix. The training function is also based on the algorithm of Levenberg-Marquardt back-propagation. Accordingly, Figure 3 indicates the inverse of the norm values of the sample neurons for better selecting and indicating the optimum hyperparameters. In this case, the optimum neurons are those that have the maximum norm quantity. Accordingly, the well-established AANN needs 25 neurons for the mapping and de-mapping layers ($l_1 = l_2 = l$) and five neurons for the bottleneck layer (h). Using the trained AANN with such hyperparameters, the residual matrix $\mathbf{E_x}$ is extracted and stored as the normalized feature matrix regarding the undamaged state of the bridge. To indicate the positive influence of data normalization, Figure 4 compares the Euclidean norms of the original modal frequencies in $\mathbf{X}$ and their residuals in $\mathbf{E_x}$. As can be seen, the norms of the modal frequencies in Figure 4(a) resemble the original values in Figure 2. This means that the use of the Euclidean norm for comparison is an accurate choice. However, as Figure 4(b) appears, the developed AANN could significantly mitigate the effect of environmental variability. In this case, the sudden sharp increases in the original modal frequencies have not only been removed, but also the amounts of the norms the residuals have considerably decreased. These conclusions verify the reliable and positive influence of the AANN-based data normalization for eliminating environmental variability. For the current state of the bridge structure in the inspection phase, the trained AANN is re-used to remove the environmental variations from the feature samples of the testing data $\mathbf{Z}$ and obtain the residual matrix $\mathbf{E_z}$.

Damage assessment

After obtaining the normalized features of the normal and current states, these are divided into segments with 10 samples. For the feature matrix of the normal condition $\mathbf{E_x}$, it is divided into 312 segments (c) so that the first 311 and last segments have 10 and 13 samples,

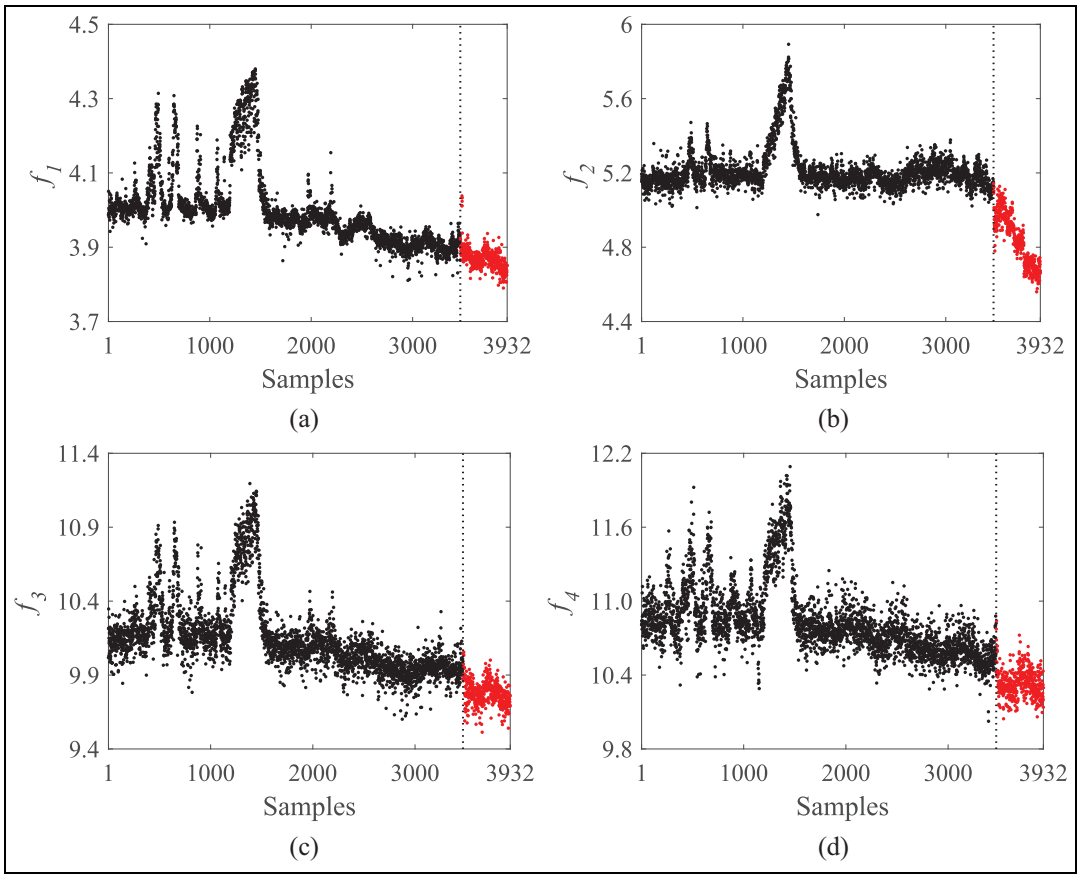

Figure 2. The modal frequencies of the Z24 bridge: (a) mode 1, (b) mode 2, (c) mode 3, and (d) mode 4.

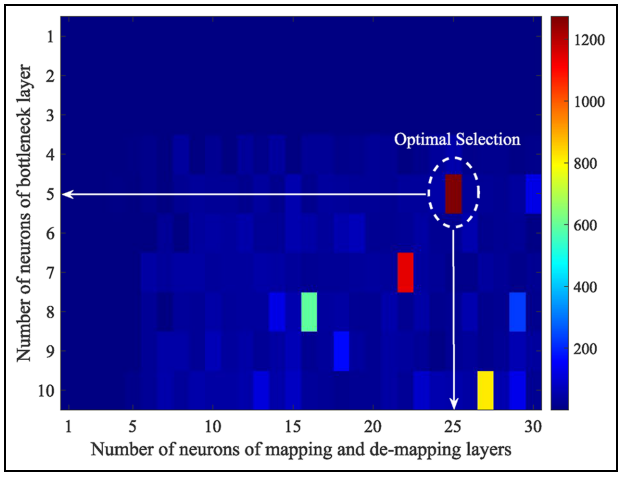

Figure 3. Determination of the optimal neurons of the hidden layers of the AANN by using the inverse of norm values for better observation.
AANN: auto-associative neural network.

respectively. Furthermore, the feature set $\mathbf{E_z}$ regarding the current state of the bridge is partitioned into 81 segments (r) in such a way that the first 80 and last segments comprised 10 and 9 samples, respectively. In the following, the procedure of distance calculation via the LDA, MKLD, and MBD is individually carried out by using the feature segments $\{\mathbf{E}_\mathbf{x}^{(1)},\ldots,\mathbf{E}_\mathbf{x}^{(312)}\}$ in order to determine the cumulative distance values (i.e., novelty scores of the undamaged condition) and make the distance vector $\mathbf{d}_{\text{nor}} = [D(\mathbf{E}_\mathbf{x}^{(1)})\ldots D(\mathbf{E}_\mathbf{x}^{(312)})]$. Such distance quantities are then applied to estimate a threshold limit for each of the proposed multivariate distance measures on the basis of the 95% confidence interval. In the next stage, the same distance calculation is implemented via the feature segments $\{\mathbf{E}_\mathbf{x}^{(1)},\ldots,\mathbf{E}_\mathbf{x}^{(312)}\}$ and $\{\mathbf{E}_\mathbf{z}^{(1)},\ldots,\mathbf{E}_\mathbf{z}^{(81)}\}$ so as to determine the novelty scores of the current state of the bridge, which are collected in $\mathbf{d}_{\text{cur}} = [D(\mathbf{E}_\mathbf{z}^{(1)})\ldots D(\mathbf{E}_\mathbf{z}^{(81)})]$.

The results of damage assessment (novelty detection) via the LDA, MKLD, and MBD are shown in Figure 5, where the horizontal arrows are indicative of the threshold limits. In this figure, the distance amounts of samples 1–347 are related to the normal condition, and the last 46 samples (348–393) belong to the current (damaged) state. Note that the distance values of samples 312–347 concerning the normal condition are related to the distance vector $\mathbf{d}_{\text{cur}}$, which are utilized to

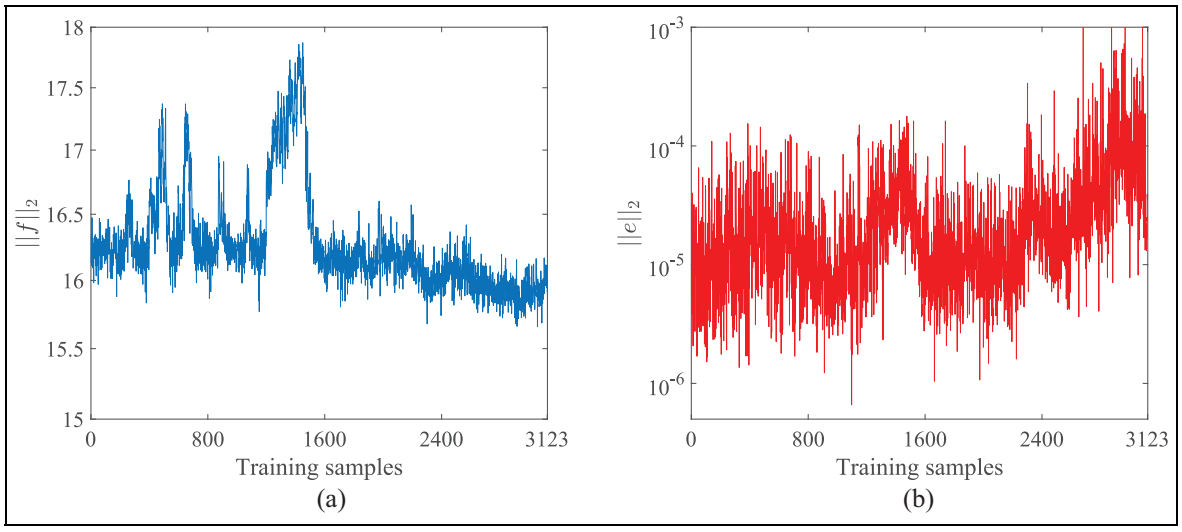

Figure 4. Comparison of the original and residual training samples: (a) the Euclidean norm of the original modal frequencies and (b) the Euclidean norm of the residuals extracted from the trained AANN.
AANN: auto-associative neural network.

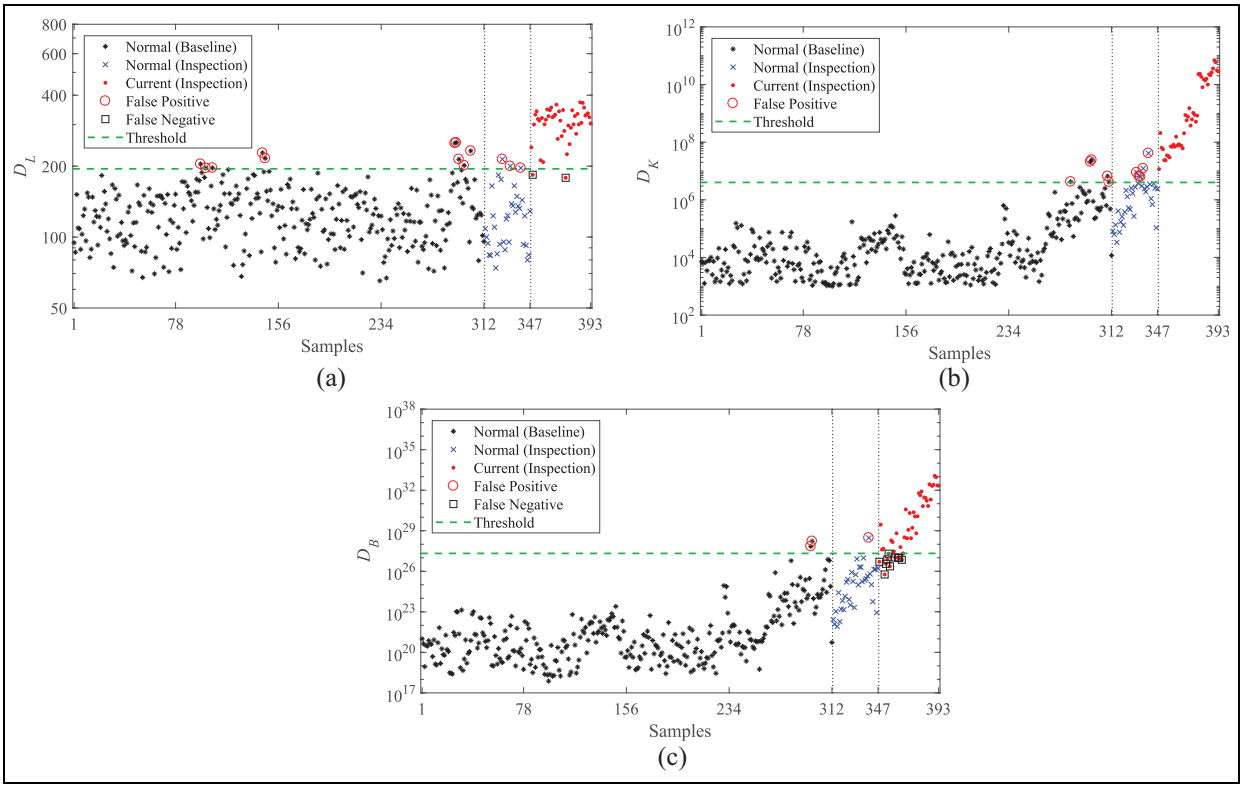

Figure 5. Damage assessment in the Z24 bridge by the proposed SHM technique: (a) LDA, (b) MKLD, and (c) MBD.
LDA: linear dissimilarity analysis; MKLD: multivariate Kullback-Leibler divergence; MBD: multivariate Bregman divergence.

validate the accuracy of data normalization and damage detection. From Figure 5, one can observe that most of the distance values or novelty scores concerning the normal condition fall below the thresholds accurately indicating the undamaged state of the bridge. On the other hand, it is seen that the majority of the distance values or novelty scores of the current state exceed the threshold limits, which imply the

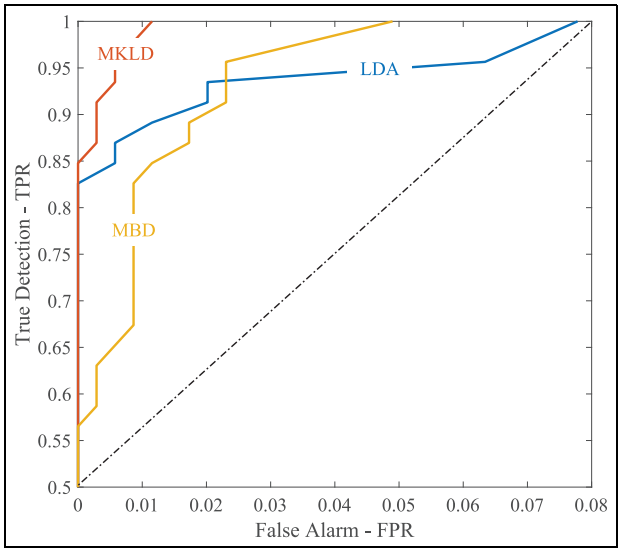

Figure 6. Performance evaluations of the proposed multivariate covariance-based distance measures.

occurrence of damage. Despite such accurate and reliable outcomes, some false alarm (false positive) and mis-detection (false negative) errors can be observable in Figure 5.

To better evaluate the performances of the multivariate distances, Figure 6 shows their receiver operating characteristic (ROC) curves. A ROC curve is a graphical tool aiming at assessing the performance of a machine learning model using the concepts of true positive rate (TPR) and false positive rate (FPR) under a given decision threshold.[52] In the context of SHM, the TPR is the probability that the method for damage assessment accurately detects damage in the structure, and the FPR means the probability that the method of interest makes a mistake in alarming the occurrence of damage, while the structure is undamaged (i.e., the probability of false positive). Accordingly, an ROC curve close to the upper left corner in the vicinity of one is indicative of a good performance, while a curve near the random guess line (the 45° line) or far away from the upper left corner implies a poor performance. With these descriptions, one can observe in Figure 6 that the MKLD outperforms the LDA and MBD. On the other hand, the LDA is better than the MBD in spite of yielding further false alarm errors.

Comparative studies

Although the results of the previous section demonstrate that the proposed SHM technique through the adjusted AANN and three covariance-based distance measures is successful in correctly detecting damage under strong temperature variability, it is important to conduct comparative studies. As mentioned, the main objective of the AANN-aided data normalization is to remove the effects of the environmental and/or operational variations and decrease the rates of false positive and false negative errors. In the first comparison, it is attempted to demonstrate how the proposed LDA, MKLD, and MBD measures operate without any data normalization. For this purpose, the actual feature sets $\mathbf{X}$ and $\mathbf{Z}$ are utilized to divide into 312 and 81 segments, respectively, as explained in section "Damage assessment."Figure 7 indicates the results of damage assessment when the AANN-aided data normalization is not incorporated.

It is observed in Figure 7(a) to (c) that the lack of using the data normalization not only increases the rate of mis-detection (false negative) but also decreases the detectability of damage of all three distances. In this case, one can see that the majority of the distance quantities of the samples 348–393, regarding the damaged state, are incorrectly under the threshold limits, particularly in Figure 7(b) and (c). Moreover, Figure 7(d) shows the ROC curves of the LDA, MKLD, and MBD without the AANN-aided data normalization. A simple comparison of these ROC curves with their counterparts in Figure 6 clearly demonstrates the positive effect of data normalization procedure on accurate and reliable damage detection.

Having considered the influence of the environmental variability, the other comparative analysis focuses on assessing the AANN-based data normalization with different neurons for the hidden layers. This comparison intends to evaluate the performance of the proposed hyperparameter selection. For this purpose, various sample neurons are applied to compare the novelty scores in terms of the total or misclassification error, which incorporates both false alarm and mis-detection errors. Due to the better performance of the MKLD against the LDA and MBD, it is used in this comparative analysis. Figure 8 indicates the percentages of the total or misclassification error in detecting damage by the MKLD under different sample neurons. As can be seen, the optimal selection of the neurons of the hidden layers ($l_1 = l_2 = l = 25$ and $h = 5$) yields the minimum rate of the total errors compared to the other samples. Note that the sixth sample neuron (i.e., 25,2,25) is the suggestion of Zhou et al.[42] and Gu et al.[43] for developing the AANN.

The other comparative analysis is concerned with the evaluation of the proposed SHM technique with its counterparts. For this purpose, two types of damage assessment techniques are considered. First, the process of damage detection is implemented by two traditional techniques based on the AANN and the MSD.[41] The AANN-based damage (novelty) detection utilizes the Euclidean norm of the residual matrix of the input

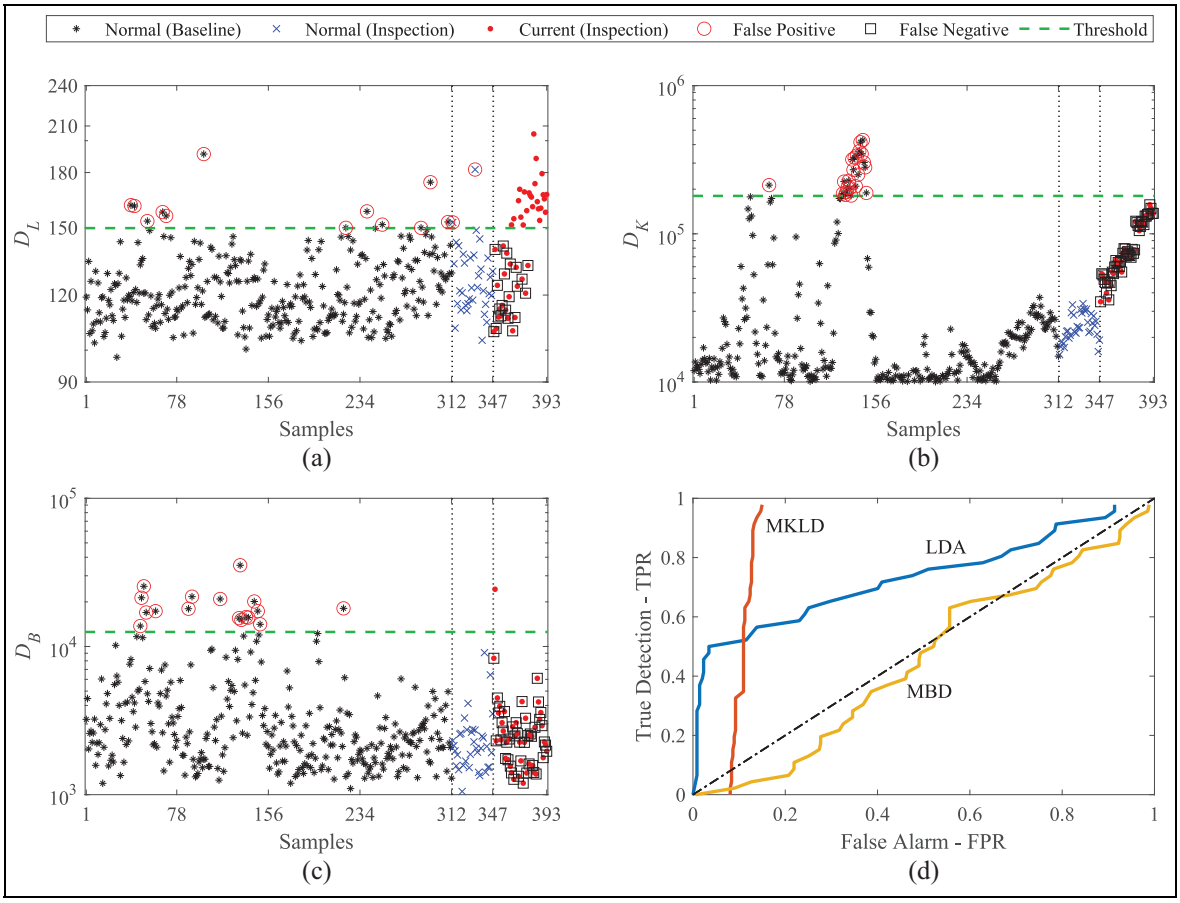

Figure 7. Damage assessment by the proposed multivariate distance measures without any data normalization: (a) LDA, (b) MKLD, (c) MBD, and (d) ROC curves.
LDA: linear dissimilarity analysis; MKLD: multivariate Kullback-Leibler divergence; MBD: multivariate Bregman divergence; ROC: receiver operating characteristic.

and output data of the AANN to obtain damage indices. Having considered the original training data $\mathbf{X}$, an AANN model is initially trained, and the model residual matrix is extracted from the input and output matrices (i.e., $\mathbf{X}$ and $\hat{\mathbf{X}}$) as expressed in Equation (3). The same process is repeated by using the original testing data $\mathbf{Z}$, in which case the trained AANN is only applied to extract a new residual matrix between new input and output matrices (i.e., $\mathbf{Z}$ and $\hat{\mathbf{Z}}$). Finally, the Euclidean norms of both residual matrices are computed to determine novelty scores for damage detection. More details on the AANN-based damage assessment are available in Figueiredo et al.[41] and Daneshvar et al.[53] Regarding the MSD, one initially needs to estimate the mean vector and covariance matrix of the training data ($\mathbf{X}$). Subsequently, n and k feature samples of the training and testing matrices are used to calculate their MSD values.[53] Second, the process of damage detection is performed by two state-of-the-art methods called unsupervised meta-learning (UML)[19] and multi-task unsupervised learning (MTUL).[14] Both methods were recently developed to detect damage under severe environmental variability. The UML method relies on four steps: an initial data analysis, data segmentation by spectral clustering, a subspace searching algorithm, and an enhanced distance metric called locally robust MSD. The MTUL method comprised three tasks: data cleaning by the density-based spatial clustering of applications with noise, data partitioning by spectral clustering, and anomaly detection via local empirical measures.

The results of damage detection via the traditional and state-of-the-art techniques are shown in Figures 9 and 10, respectively. In these figures, the horizontal lines are the threshold limits obtained from the 95% confidence interval of the damage (novelty) indices of the training features regarding the normal state of the bridge. From Figure 9, it can be seen that the same patterns of the sharp increases in modal frequencies (see Figure 2) still exist in the outputs (i.e., damage indices) of the traditional techniques. This means that the environmental variability seriously affects them, leading to large false-positive errors. Moreover, it is

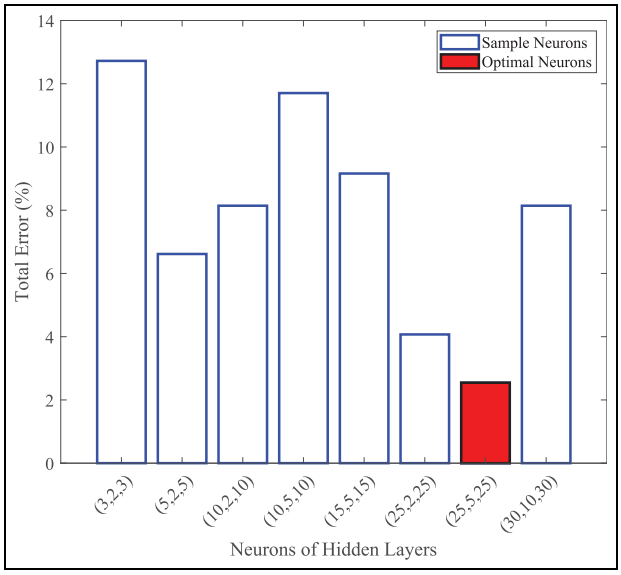

Figure 8. Comparison of the different neurons of the hidden layers based on the total error (Note: The first, second, and third numbers are related to the numbers of the mapping, bottleneck, and de-mapping layers.).

seen that the MSD yields more false-negative errors than the AANN. This indicates the low damage detectability of the MSD under strong environmental variations. Compared to Figure 5, one can conclude that the proposed SHM technique is superior to the AANN and MSD in terms of dealing with environmental variability and presenting higher damage detectability.

Regarding the state-of-the-art techniques, that is, UML and MTUL, as Figure 10 reveals, both techniques could properly mitigate the influence of the environmental variability so that the sharp increases in the modal frequencies of the training samples no longer exist. This indicates the robustness of these techniques to environmental variability. Due to these performances, both of them could provide reliable damage detectability with small false-positive and false-negative errors compared to the AANN- and MSD-based damage detection techniques. For more evaluation, Figure 11 compares the proposed SHM method with the traditional and state-of-the-art techniques in terms of the number of misclassification (total) errors. For a better presentation and interpretation, the vertical axis of this figure is shown in a logarithmic format. As expected, the traditional techniques yielded the maximum number of misclassification errors, especially the MSD. Although both the proposed and state-of-the-art methods could address the challenge of environmental variability, it is seen in Figure 11 that the proposed SHM method yields fewer misclassification errors compared to the UML and MTUL. This verifies the positive effects of feature segmentation and the use of a few damage indices for novelty detection.

All the previous results are based on the training ratio of 90%. As the final comparison, the performances of the proposed SHM technique and three covariance-based distance measures are investigated under a new training ratio equal to 75%. Accordingly, the training matrix is comprised of 2602 modal frequencies of the undamaged condition, while the remaining 25% of the modal frequencies of this condition (i.e., the samples 2603–3470) along with all modal frequencies of the damaged state are used in the testing matrix. Subsequently, the process of data normalization via an AANN is performed to remove the environmental variations and make new feature matrices $\mathbf{E}_x$

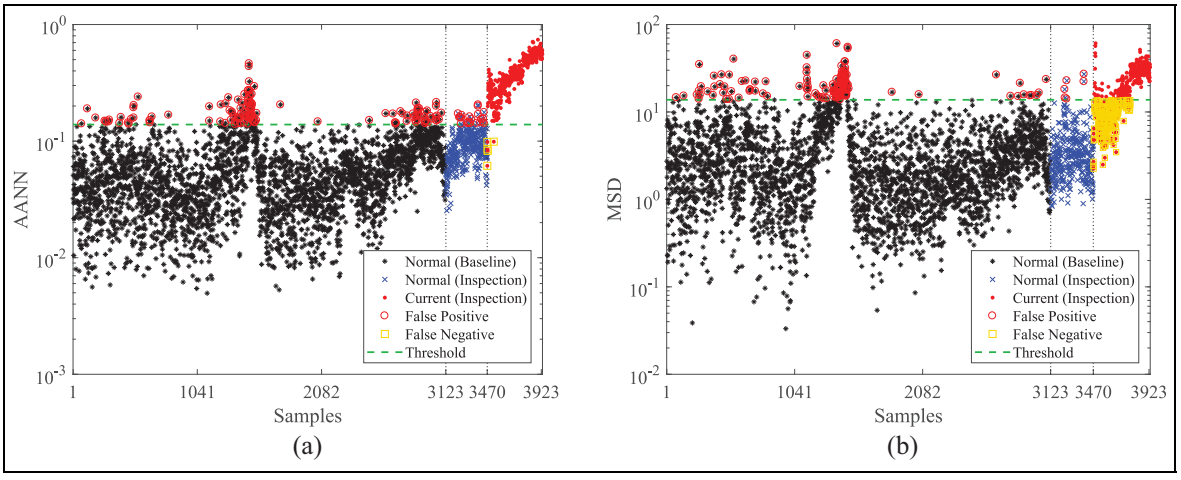

Figure 9. Damage assessment by the traditional SHM techniques: (a) AANN and (b) MSD.
AANN: auto-associative neural network; MSD: Mahalanobis-squared distance; SHM: structural health monitoring.

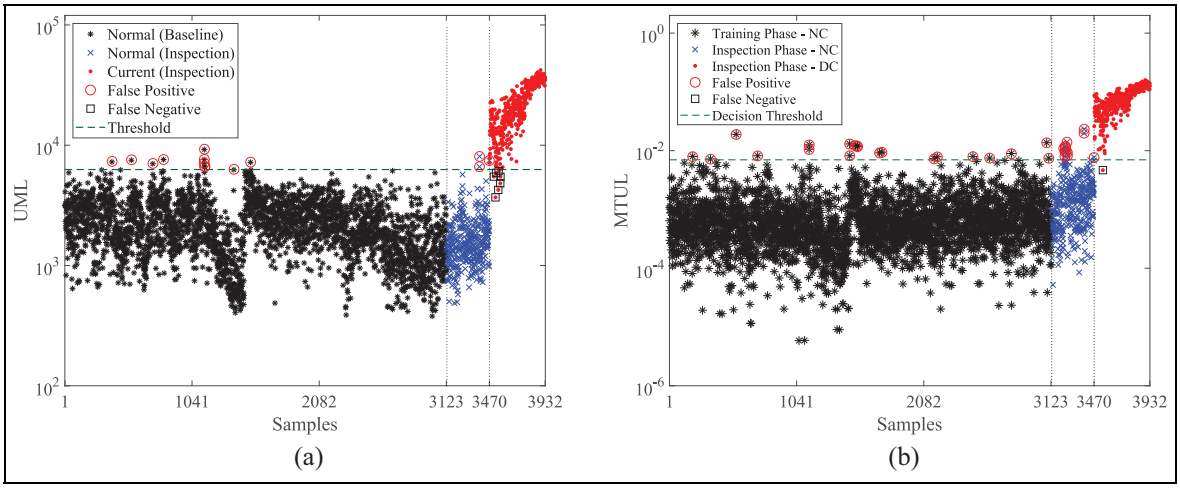

Figure 10. Damage assessment by the state-of-the-art SHM techniques: (a) UML and (b) MTUL.
MTUL: multi-task unsupervised learning; UML: unsupervised meta-learning; SHM: structural health monitoring.

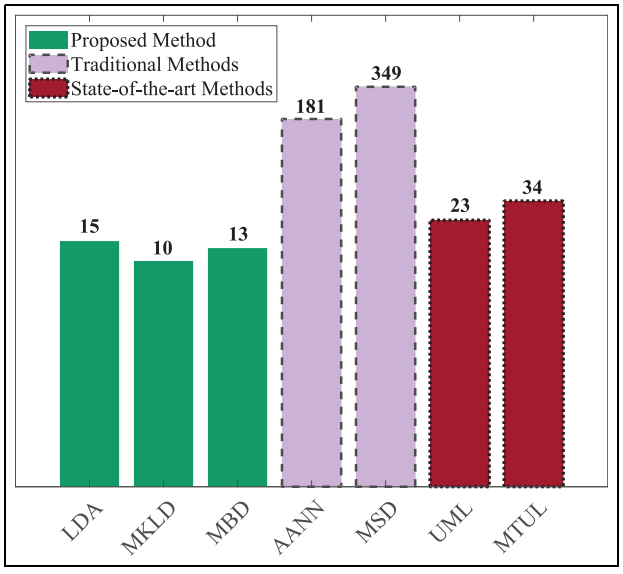

Figure 11. Comparison of the proposed method with the traditional and state-of-the-art techniques in terms of the number and misclassification errors (i.e., the vertical axis is a logarithmic format).

and $\mathbf{E}_z$. Using Algorithm 1, the neurons of the mapping, bottleneck, and de-mapping layers are equal to 21, 4, and 21, respectively. Figure 12(a) to (c) shows the results of damage assessment by the LDA, MKLD, and MBD, respectively. Furthermore, Figure 12(d) illustrates the numbers and percentages of the total errors related to the training ratios of 90% and 75%. In this figure, the amount on top of each bar indicates the number of total errors. The observations in Figure 12(a) to (c) and the comparison with Figure 5 obviously demonstrate that the reduction in the training samples increases the rate of false-positive, particularly in the validation data. The same conclusion can be seen in Figure 12(d), where the numbers and percentages of the total errors significantly increase by reducing the number of training samples. These observations confirm the importance of using sufficient feature samples for making an appropriate training set in order to increase the reliability of novelty detection.

Conclusion

This article proposed an innovative data-based SHM technique consisting of data normalization and distance-based novelty detection. The process of data normalization was performed by an adjusted AANN with the aid of a new hyperparameter selection strategy. In addition, three multivariate covariance-based distances were suggested to compute novelty scores for damage assessment by using the normalized features extracted from the AANN-aided data normalization. The well-known Z24 bridge was considered to verify the effectiveness and reliability of the proposed SHM technique, along with several comparative analyses.

The results demonstrated that the proposed data normalization approach could highly reduce the effect of strong environmental (temperature) variations in the bridge modal frequencies. The lack of considering this approach significantly increased the rates of false positive and false negative errors. It was observed that the proposed hyperparameter selection algorithm could choose the optimum neurons of the hidden layers of the AANN with the minimum error. All the proposed covariance-based distance measures were successful in detecting damage with inconsiderable false positive and false negative errors. The comparative analyses among

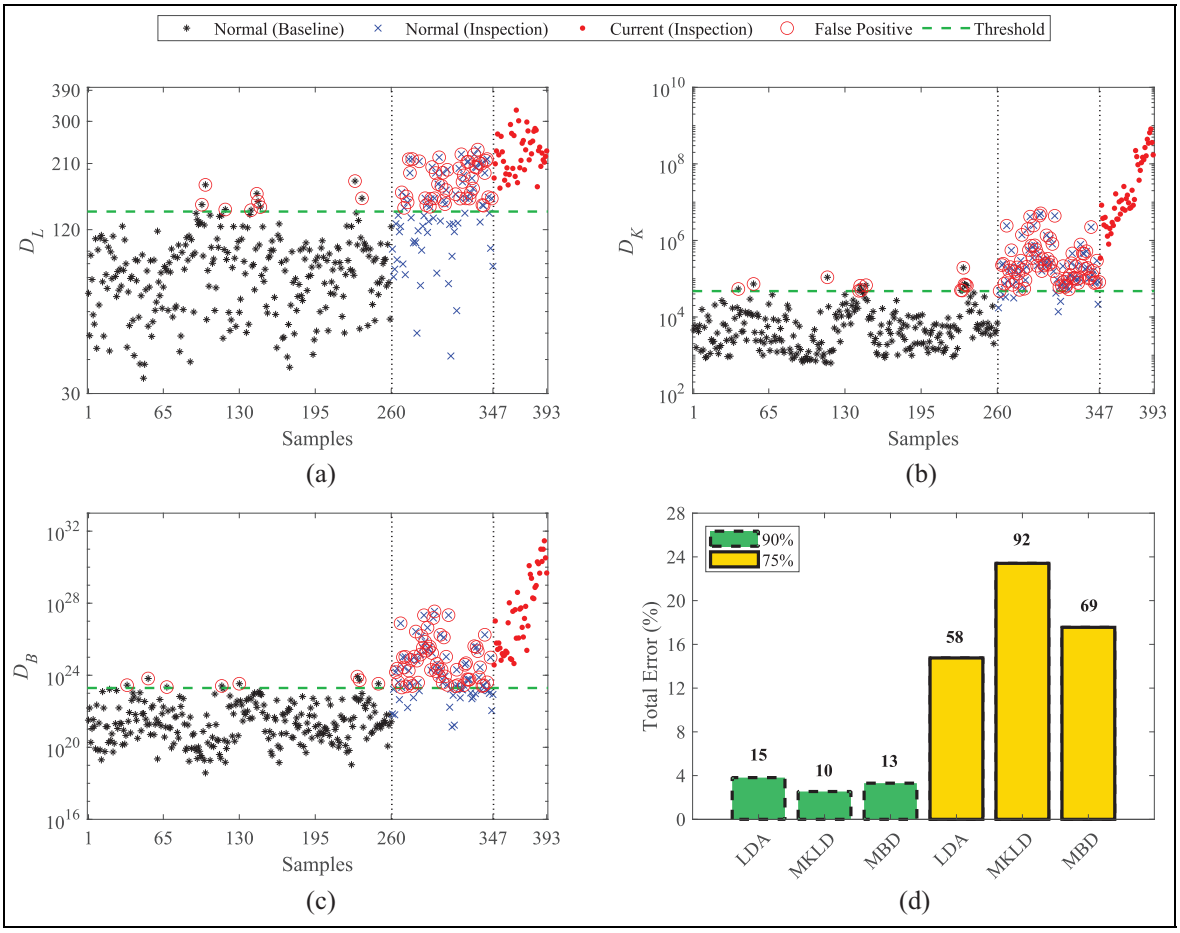

Figure 12. Damage assessment by the proposed multivariate covariance-based distance measures by using the training rate of 75%: (a) LDA, (b) MKLD, (c) MBD, and (d) total errors.
LDA: linear dissimilarity analysis; MKLD: multivariate Kullback-Leibler divergence; MBD: multivariate Bregman divergence.

them demonstrated that the MKLD outperformed the LDA and MBD. It was also observed that all three distance measures were superior to the traditional damage detection techniques based on the AANN and MSD. Although both the proposed and state-of-the-art (i.e., UML and MTUL) techniques could properly mitigate the environmental variability, the SHM method presented in this article could yield smaller misclassification (total) errors compared to the state-of-the-art techniques. This conclusion indicates the positive influence of the proposed feature segmentation before novelty detection. Eventually, it was demonstrated that the reduction in the number of training samples had a negative effect on the performance of the proposed SHM technique. In this case, it is necessary to incorporate relatively large feature samples of the normal condition in order to capture all possible environmental and/or operational variability conditions.

Declaration of conflicting interests

The author(s) declared no potential conflicts of interest with respect to the research, authorship, and/or publication of this article.

Funding

The author(s) received no financial support for the research, authorship, and/or publication of this article.

ORCID iD

Hashem Shariatmadar https://orcid.org/0000-0001-5966-3317

References

1. Cawley P. Structural health monitoring: closing the gap between research and industrial deployment. *Struct Health Monit* 2018; 17: 1225–1244.

2. Zhou X-Q, Xia Y and Weng S. L1 regularization approach to structural damage detection using frequency data. *Struct Health Monit* 2015; 14: 571–582.
3. Entezami A, Shariatmadar H and Sarmadi H. Structural damage detection by a new iterative regularization method and an improved sensitivity function. *J Sound Vib* 2017; 399: 285–307.
4. Rezaiee-Pajand M, Sarmadi H and Entezami A. A hybrid sensitivity function and Lanczos bidiagonalization-Tikhonov method for structural model updating: application to a full-scale bridge structure. *Appl Math Model* 2021; 89: 860–884.
5. Malekloo A, Ozer E, AlHamaydeh M, et al. Machine learning and structural health monitoring overview with emerging technology and high-dimensional data source highlights. *Struct Health Monit* 2022; 21: 1906–1955.
6. Sarmadi H and Yuen K-V. Early damage detection by an innovative unsupervised learning method based on kernel null space and peak-over-threshold. *Comput Aided Civ Inf* 2021; 36: 1150–1167.
7. Figueiredo E and Brownjohn J. Three decades of statistical pattern recognition paradigm for SHM of bridges. *Struct Health Monit* 2022; 21: 3018–3054.
8. Lynch JP, Sohn H and Wang ML. *Sensor Technologies for Civil Infrastructures: Volume 1: Sensing Hardware and Data Collection Methods for Performance Assessment*. Cambridge, MA: Elsevier, 2022.
9. Feng D and Feng MQ. Computer vision for SHM of civil infrastructure: From dynamic response measurement to damage detection – A review. *Eng Struct* 2018; 156: 105–117.
10. Sarmadi H, Entezami A, Yuen K-V, et al. Review on smartphone sensing technology for structural health monitoring. *Measurement* 2023; 223: 113716.
11. Ay AM and Wang Y. Structural damage identification based on self-fitting ARMAX model and multi-sensor data fusion. *Struct Health Monit* 2014; 13: 445–460.
12. Kopsaftopoulos FP and Fassois SD. A vibration model residual-based sequential probability ratio test framework for structural health monitoring. *Struct Health Monit* 2015; 14: 359–381.
13. Entezami A, Shariatmadar H and Karamodin A. Data-driven damage diagnosis under environmental and operational variability by novel statistical pattern recognition methods. *Struct Health Monit* 2019; 18: 1416–1443.
14. Entezami A, Sarmadi H, Behkamal B, et al. On continuous health monitoring of bridges under serious environmental variability by an innovative multi-task unsupervised learning method. *Struct Infrastruct Eng*. Epub ahead of print 04 August 2022. DOI: 10.1080/15732479.2023.2166538.
15. Pimentel MA, Clifton DA, Clifton L, et al. A review of novelty detection. *Signal Process* 2014; 99: 215–249.
16. Cha Y-J and Wang Z. Unsupervised novelty detection-based structural damage localization using a density peaks-based fast clustering algorithm. *Struct Health Monit* 2018; 17: 313–324.
17. Daneshvar MH and Sarmadi H. Unsupervised learning-based damage assessment of full-scale civil structures under long-term and short-term monitoring. *Eng Struct* 2022; 256: 114059.
18. Entezami A, Shariatmadar H and De Michele C. Non-parametric empirical machine learning for short-term and long-term structural health monitoring. *Struct Health Monit* 2022; 21: 2700–2718.
19. Entezami A, Sarmadi H and Behkamal B. Long-term health monitoring of concrete and steel bridges under large and missing data by unsupervised meta learning. *Eng Struct* 2023; 279: 115616.
20. Zhou Y, Shu X, Bao T, et al. Dam safety assessment through data-level anomaly detection and information fusion. *Struct Health Monit* 2023; 22: 2002–2021.
21. Sarmadi H, Entezami A and De Michele C. Probabilistic data self-clustering based on semi-parametric extreme value theory for structural health monitoring. *Mech Syst Sig Process* 2023; 187: 109976.
22. Entezami A, Sarmadi H and Behkamal B. A novel double-hybrid learning method for modal frequency-based damage assessment of bridge structures under different environmental variation patterns. *Mech Syst Sig Process* 2023; 201: 110676.
23. Wang Z, Yang D-H, Yi T-H, et al. Eliminating environmental and operational effects on structural modal frequency: a comprehensive review. *Struct Contr Health Monit* 2022; 29: e3073.
24. Han Q, Ma Q, Xu J, et al. Structural health monitoring research under varying temperature condition: a review. *J Civ Struct Health Monit* 2021; 11: 149–173.
25. Kita A, Cavalagli N and Ubertini F. Temperature effects on static and dynamic behavior of Consoli Palace in Gubbio, Italy. *Mech Syst Sig Process* 2019; 120: 180–202.
26. Sarmadi H and Yuen K-V. Structural health monitoring by a novel probabilistic machine learning method based on extreme value theory and mixture quantile modeling. *Mech Syst Sig Process* 2022; 173: 109049.
27. Comanducci G, Magalhães F, Ubertini F, et al. On vibration-based damage detection by multivariate statistical techniques: application to a long-span arch bridge. *Struct Health Monit* 2016; 15: 505–524.
28. Farreras-Alcover I, Chryssanthopoulos MK and Andersen JE. Regression models for structural health monitoring of welded bridge joints based on temperature, traffic and strain measurements. *Struct Health Monit* 2015; 14: 648–662.
29. Gianesini BM, Cortez NE, Antunes RA, et al. Method for removing temperature effect in impedance-based structural health monitoring systems using polynomial regression. *Struct Health Monit* 2021; 20: 202–218.
30. Roberts C, Cava DG and Avendaño-Valencia LD. Addressing practicalities in multivariate nonlinear regression for mitigating environmental and operational variations. *Struct Health Monit* 2022; 22: 1237–1255.
31. Behkamal B, Entezami A, De Michele C, et al. Investigation of temperature effects into long-span bridges via

hybrid sensing and supervised regression models. *Remote Sens* 2023; 15: 3503.
32. Behkamal B, Entezami A, De Michele C, et al. Elimination of thermal effects from limited structural displacements based on remote sensing by machine learning techniques. *Remote Sens* 2023; 15: 3095.
33. Maes K, Van Meerbeeck L, Reynders EPB, et al. Validation of vibration-based structural health monitoring on retrofitted railway bridge KW51. *Mech Syst Sig Process* 2022; 165: 108380.
34. Reynders E, Wursten G and De Roeck G. Output-only structural health monitoring in changing environmental conditions by means of nonlinear system identification. *Struct Health Monit* 2014; 13: 82–93.
35. Soo Lon Wah W, Chen Y-T, Roberts GW, et al. Separating damage from environmental effects affecting civil structures for near real-time damage detection. *Struct Health Monit* 2018; 17: 850–868.
36. Silva M, Santos A, Santos R, et al. Deep principal component analysis: an enhanced approach for structural damage identification. *Struct Health Monit* 2019; 18: 1444–1463.
37. Daneshvar MH, Sarmadi H and Yuen K-V. A locally unsupervised hybrid learning method for removing environmental effects under different measurement periods. *Measurement* 2023; 208: 112465.
38. Sarmadi H, Entezami A and Magalhães F. Unsupervised data normalization for continuous dynamic monitoring by an innovative hybrid feature weighting-selection algorithm and natural nearest neighbor searching. *Struct Health Monit* 2023; 22: 4005–4026.
39. Kramer MA. Autoassociative neural networks. *Comput Chem Eng* 1992; 16: 313–328.
40. Sarmadi H. Investigation of machine learning methods for structural safety assessment under variability in data: comparative studies and new approaches. *J Perform Constr Facil* 2021; 35: 04021090.
41. Figueiredo E, Park G, Farrar CR, et al. Machine learning algorithms for damage detection under operational and environmental variability. *Struct Health Monitor* 2011; 10: 559–572.
42. Zhou HF, Ni YQ and Ko JM. Structural damage alarming using auto-associative neural network technique: exploration of environment-tolerant capacity and setup of alarming threshold. *Mech Syst Sig Process* 2011; 25: 1508–1526.
43. Gu J, Gul M and Wu X. Damage detection under varying temperature using artificial neural networks. *Struct Contr Health Monit* 2017; 24: e1998.
44. Jin S-S and Jung H-J. Vibration-based damage detection using online learning algorithm for output-only structural health monitoring. *Struct Health Monit* 2018; 17: 727–746.
45. Kano M, Nagao K, Hasebe S, et al. Comparison of multivariate statistical process monitoring methods with applications to the Eastman challenge problem. *Comput Chem Eng* 2002; 26: 161–174.
46. Entezami A, Shariatmadar H and Mariani S. Fast unsupervised learning methods for structural health monitoring with large vibration data from dense sensor networks. *Struct Health Monit* 2020; 19: 1685–1710.
47. Entezami A, Sarmadi H and De Michele C. Probabilistic damage localization by empirical data analysis and symmetric information measure. *Measurement* 2022; 198: 111359.
48. Mei Q and Gül M. A crowdsourcing-based methodology using smartphones for bridge health monitoring. *Struct Health Monit* 2019; 18: 1602–1619.
49. Kulis B, Sustik M and Dhillon I. Learning low-rank kernel matrices. In: *Proceedings of the 23rd international conference on machine learning* 2006, Pittsburgh, Pennsylvania, pp. 505–512.
50. Sarmadi H, Entezami A, Salar M, et al. Bridge health monitoring in environmental variability by new clustering and threshold estimation methods. *J Civ Struct Health Monit* 2021; 11: 629–644.
51. Peeters B and De Roeck G. One-year monitoring of the Z24-Bridge: environmental effects versus damage events. *Earthquake Eng Struct Dyn* 2001; 30: 149–171.
52. Stull CJ, Hemez FM and Farrar CR. On assessing the robustness of structural health monitoring technologies. *Struct Health Monit* 2012; 11: 712–723.
53. Daneshvar MH, Gharighoran A, Zareei SA, et al. Early damage detection under massive data via innovative hybrid methods: application to a large-scale cable-stayed bridge. *Struct Infrastruct Eng* 2021; 17: 902–920.